Friction **11**(6): 865–880 (2023)
https://doi.org/10.1007/s40544-022-0618-5
ISSN 2223-7690
CN 10-1237/TH
RESEARCH ARTICLE

Concept of radial slippage propagation triggering self-loosening and optimisation design of novel anti-loosening structures

Hao GONG, Jianhua LIU*, Huihua FENG, Jiayu HUANG
Beijing Institute of Technology, School of Mechanical Engineering, Beijing 100081, China
Received: 03 November 2021 / Revised: 23 January 2022 / Accepted: 08 March 2022

Abstract: Self-loosening of bolted joints can occur in a vibration environment, and it may induce bolt fatigue fracture with catastrophic consequences. It is essential to clarify the self-loosening mechanism, based on which novel anti-loosening thread structures can be developed. In this paper, we propose the concept of radial slippage propagation and provide new insights into the self-loosening process. The new theory states that the slippage along the radial direction of the thread surface induces more slippage areas (slippage propagation), and self-loosening occurs due to the dynamic evolution and propagation of contact states on the thread and bearing surfaces with an increase in the number of vibration cycles. Finite element analysis (FEA) was used to validate the propagation process of slippage areas on the thread surface. A novel bolted joint with step thread engagement was developed, which could prevent the occurrence of relative motion of the external and internal threads in the radial direction and thus block slippage propagation. A three-dimensional (3D) finite element model (FEM) of the novel thread structure was established, and a test specimen was manufactured using two special tools. FEA and experiments validated its superior anti-loosening and anti-fatigue performances, and the convenience of installation and removal. Experimental validation of the radial slippage propagation theory and the performance optimisation of the step-thread structure should be performed in the future.

Keywords: bolted joint; self-loosening; slippage propagation; step thread; transversal vibration

1 Introduction

Bolted joints are widely applied to fasten two or more separated components owing to the ease of installation and dismantlement for repairment and low cost [1]. Nevertheless, loosening can occur when bolted joints are exposed to an external vibration and impact environment [2, 3]. Loosening directly leads to preload decrease and induces fatigue fracture of bolts, thus initiating catastrophic safety accidents in some circumstances. For example, in 2010, a collapse accident at Space Lost [4], in an amusement park in eastern Shenzhen, China, occurred due to loosening, which triggered the fatigue fracture of bolts, resulting in six deaths and 10 injuries. To increase the safety and reliability of mechanical systems, the exploration of loosening mechanisms and anti-loosening methods has never stopped.

Gong et al. [5] reviewed the research on loosening, and it was concluded that loosening is divided into non-rotational and rotational loosening. For the former, the preload in a bolted joint is reduced with no relative rotation of the nut and bolt. Stress redistribution, cyclic plastic deformation, embedding loss, stress relaxation, and creep and embedding loss are the main factors that cause non-rotational loosening [6–12]. The latter, which is also called self-loosening, implies a rotation of the nut and bolt along the loosening direction. In comparison, self-loosening can result in a consecutive preload decrease until the fatigue fracture of bolt occurs, or there is no preload in the bolt, thus generating greater harm. In 1969, the German engineer

* Corresponding author: Jianhua LIU, E-mail: jeffliu@bit.edu.cn

Junker [13] developed a machine and first applied cyclic transversal vibration (vertical to the bolt axis) to bolted joints in experiments. It was observed that large-scale and continued self-loosening would occur under cyclic transversal vibration, compared with cyclic longitudinal vibration [14]. At that time, the complete slippage theory was developed to illustrate the loosening process, which will be introduced in detail in Section 2. Owing to the lack of effective methods for the actual observation of contact states on the thread and bearing surfaces under transversal vibration, the complete slippage theory was widely accepted for a long time. In 2002, two American scholars, Pai and Hess [15, 16] established a three-dimensional (3D) finite element model (FEM) of a bolted joint and simulated the cyclic transversal vibration applied to a bolted joint. The contact states on the thread and bearing surfaces at each vibration moment were clearly observed. They challenged the classical theory and proposed the local slippage accumulation theory to illustrate the self-loosening process. The details of the local slippage accumulation theory are also presented in Section 2. Subsequently, further research has validated the reliability of the new theory explaining self-loosening [17, 18]. Gong and Liu [19] and Dinger and Friedrich [20] defined a parameter to quantitatively describe the self-loosening due to the local slippage accumulation. Recently, Gong et al. [21, 22] established the modified Iwan models to represent the local slippage accumulation. These developments increased the understanding of self-loosening according to the local slippage accumulation theory.

Many anti-loosening structures or products are used to prevent self-loosening in engineering applications [23]. Common anti-loosening structures can be divided into two main forms: washers and nuts. The former includes plain washers, spring washers, Belleville washers, and wedge washers. It has been demonstrated that plain washers and spring washers [24, 25] barely have anti-loosening abilities. The former was designed to protect the surfaces of the clamped plates, while the latter was suggested to be moved from the national standardisation. Belleville washers or wedge washers installed in bolted joints show some degree of anti-loosening ability [26, 27] but cannot completely inhibit it. The latter mainly consists of wedge locking nuts, prevailing torque nuts, eccentric double nuts, and double nuts. They have been demonstrated to provide superior anti-loosening abilities [28–31]. In the transversal vibration experiment or finite element (FE) simulation, the preloads decrease very slowly or remain almost unchanged with the increase in vibration cycles. However, this type of anti-loosening structure has an apparent disadvantage, that is, higher tightening torque is required to obtain the objective preload, compared with the normal bolted joint. Furthermore, some novel anti-loosening structures have been proposed. For example, Ranjan et al. [32] changed the geometrical shape of the external thread to be a cubic function of the rotation. The mismatch between the novel bolt and normal nut resulted in interference, and larger torque was needed to conquer the interference. Sase et al. [33, 34] developed a new bolt structure named "step-lock bolt" (SLB). The SLB had several steps where the degree of lead angle was zero at the circumference of the thread. Sun et al. [35] proposed a novel bolt structure, which had a matched spherical gasket. An increased preload would be generated when the transversal loading increased. The anti-loosening abilities and tightening performance of these structures must be further validated before widespread applications.

The above review summarises the research progress on loosening mechanisms and anti-loosening methods. The loosening mechanism based on the local slippage accumulation theory has obtained mainstream acceptance. However, this theory can only explain the rotational loosening process in a simplified way. The actual rotational loosening process is more complicated; and thus, the slippage behaviour and its evolution on the contact surfaces require further investigation. Moreover, most of the anti-loosening structures applied with excellent performance in preventing loosening show inconvenience of installation and disassembly or poor fatigue resistance. Novel anti-loosening structures with convenient tightening and dismantlement, good anti-loosening, and anti-fatigue performance require further exploration. These were the motivations for this study. In this paper, we propose the concept of radial slippage propagation to further reveal the rotational loosening process. Based on the new theory, it is found that self-loosening is developed by the dynamical evolution of contact states: from minor slippage

propagation to local slippage accumulation, finally developing to complete slippage. This provides new insights into the mechanism of rotational loosening. In addition, a novel anti-loosening structure is proposed. The experimental and finite element analysis (FEA) results validate its excellent anti-loosening and fatigue resistance performance and convenience of installation.

2 Classical slippage theories to explain self-loosening

Slippage movements on the bearing and thread surfaces form the basis of self-loosening. Two different slippage modes (or slippage theories) have been developed to reveal the process of self-loosening under transversal vibration: the complete slippage theory and the local slippage accumulation theory. This section introduces in detail the two theories, which lay the foundation for understanding the novel slippage theory in Section 3.

Cyclic transversal vibration is usually applied to a clamped plate, as shown in Fig. 1. Empirically, transversal vibration with a larger amplitude will cause more severe self-loosening. For example, in a quarter-cycle, the transversal force F increases gradually and reaches the maximum F_g at the point a_6 (or the dead point). The slipping areas on the bearing and thread surfaces also increase gradually as the transversal force increases from the coordinate origin, as shown in Fig. 2. It can be found that complete slippage on the thread and bearing surfaces occurs when the transversal force is larger than F_f (at the point a_5). The complete slippage theory states that self-loosening cannot appear unless the vibration amplitude is greater than F_f. This is because all the contact areas will slip when the transversal force reaches the extreme, fully overcoming the bearing friction torque T_b and thread friction torque T_t. The relative rotational movement of the external and internal threads opposite the assembly direction appears and continues owing to the pitch torque T_p. This is an early explanation of self-loosening based on the classical friction law and has been widely accepted for a long time.

However, it was shown that self-loosening also occurred without complete slippage when the transversal force reaches its maximum. This means that the self-loosening condition caused by complete slippage is sufficiently strict. Subsequently, another slippage theory named "local slippage accumulation theory" was proposed by Pai and Hess [15, 16] to provide a new explanation for self-loosening. The concept of the local slippage has not been strictly defined in previous research. In general, slipping occurred in the partial contact areas (incomplete slippage) is regarded as a local slippage. In the local slippage accumulation theory, the vibration amplitude (the maximum transversal force) is equal to F_d or F_e, as shown in Fig. 1. More than half of the contact areas are in a slippage state, and the residual contact areas are in a sticking state when the transversal force reaches the maximum value in the $+x$ direction, as shown in Fig. 3(a). Within the other half of the vibration cycle, more than half of the contact areas are in the slippage state when the transversal force reaches the maximum value in the $-x$ direction, as

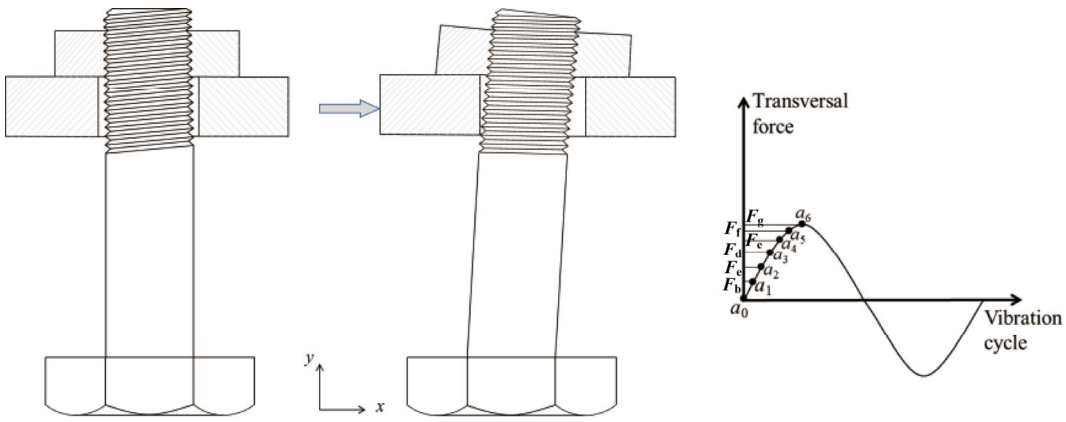

Fig. 1 Cyclic transversal vibration is employed to a bolted joint along x-axis (a_0 denotes the original point; a_1–a_6 denote transversal vibrational points in a quarter-cycle, and F_b–F_g denote the corresponding transversal forces).

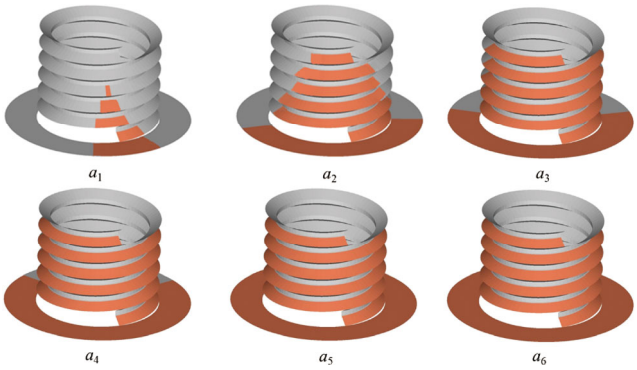

Fig. 2 Evolution of slipping areas on the bearing and thread surfaces within a quarter vibration cycle.

shown in Fig. 3(b). Over a complete vibration cycle, no constant-sticking area appears, and all the contact areas slip, as shown in Fig. 3(c). Self-loosening proceeds by this type of incomplete slippage containing no constant-sticking area within a complete vibration cycle. Herein, we define the local slippage as an incomplete slippage containing no constant-sticking area within a complete vibration cycle. Incomplete slippage containing a constant-sticking area within a complete vibration cycle is defined as minor slippage. According to the local slippage accumulation theory, minor slippage cannot cause continued self-loosening. The critical amplitude corresponding to self-loosening is the exact amplitude resulting in local slippage accumulation on the bearing and thread surfaces.

3 Radial slippage propagation theory

The above two slippage theories are not contradictory; and they explain the process of self-loosening at different magnitudes of vibration amplitude. When the amplitude is sufficiently large to cause complete slippage on the thread and bearing surfaces at the positions of maximum transversal force, the complete slippage theory explains the self-loosening process. When the amplitude can cause local slippage on the thread and bearing surfaces at the positions of the maximum transversal force, the local slippage accumulation theory clarifies the self-loosening process. However, based on the modified Iwan model [21] and FEA [22], we found that not all minor slippages can initiate self-loosening. Minor slippage with a small constant-sticking area within a complete vibration cycle at the initial vibration cycles can also expand to local slippage and complete slippage as the number of vibration cycles is increased, finally resulting in self-loosening. Therefore, the "radial slippage propagation theory" is proposed to provide a new insight into the self-loosening process under transversal vibration. The relationship between the slippage theory and other existing theories is shown in Fig. 4.

Similarly, a cyclic transversal vibration along the x-axis was applied to the clamped plate, as shown in Fig. 5(a). The thread surfaces of one pitch and bearing surface are analysed. The radial and circumferential directions of the bearing and thread surfaces are shown in Fig. 5(b). When the transversal force is increased and is at its maximum along the $+x$ direction, the minor thread contact areas slip first along the radial direction of the thread surface. It has been demonstrated that the radial slippage occurring periodically causes the stored energy releasing and being transformed to power such that slipping occurs along the spiral direction (i.e. circumferential direction) [21, 22]. Consequently, more slipping areas appear in the

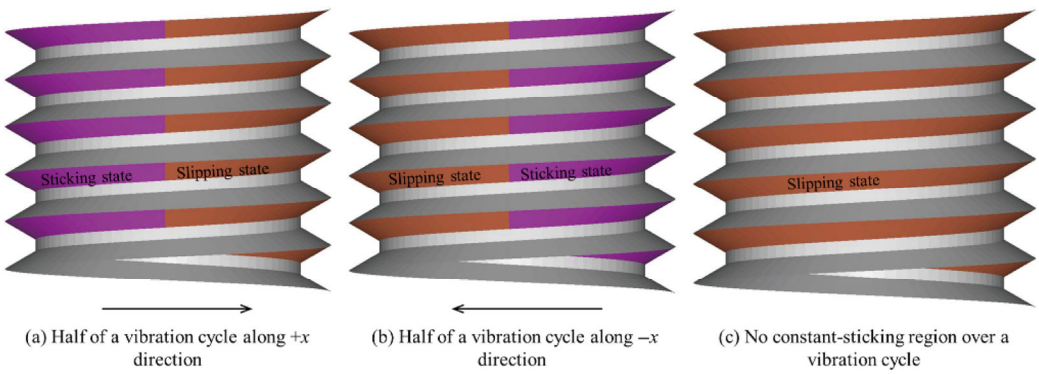

Fig. 3 Local slippage accumulation theory.

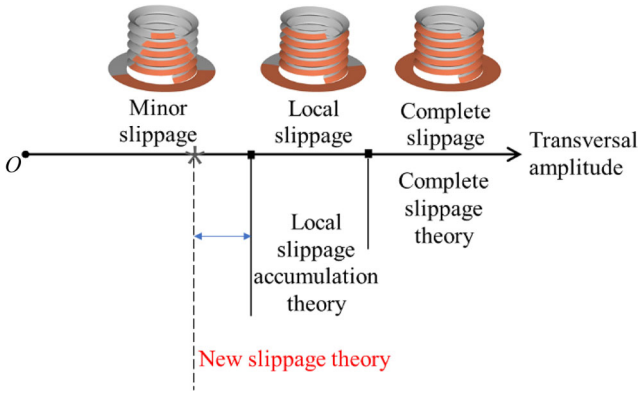

Fig. 4 Relationship between the new slippage theory and other existing theories.

following vibration cycles. Moreover, the decrease in preload owing to slippage behaviour on the thread surface may further aggravate the slippage propagation. For the bearing surface, thread slippage generates torque between the thread and bearing surfaces. This torque and the transversal force induce the release of the stored internal energy on the bearing surface, and the bearing contact areas propagate gradually. The decrease in preload also exacerbates the slippage propagation on the bearing surface. The above slippage behaviour is defined as the "radial slippage propagation theory". From Fig. 5(b), we can observe that minor slippage on the thread and bearing surfaces will develop to local slippage by radial slippage propagation as the transversal vibration proceeds.

Figure 6 shows the complete self-loosening process of a bolted joint subjected to a medium vibration causing minor slippage on the bearing and thread surfaces with a small constant-sticking area within a complete vibration cycle. When the local slippage resulting from the propagation of minor slippage occurs on the bearing and thread surfaces, small rotational loosening will appear based on the local slippage accumulation theory. The preload thus decreases, providing a positive feedback to the slippage behaviour on the contact interfaces. Thereby, more contact areas will slip, and the self-loosening will accelerate. Finally, local slippage will expand to complete slippage when the vibration cycle increases continuously, and large-scale self-loosening will occur. Herein, a 3D FEM of a regular bolted joint was built, as shown in Fig. 7(a). A periodic transversal vibration applied to the bolted joint was simulated. The nominal diameter and pitch of bolt and nut are 10 and 1.5 mm, respectively. The material is steel #1045 with the elastic modulus of 206 GPa and Poisson's ratio of 0.3. The friction coefficients of all the contact interfaces were set to 0.15. The preload was tightened to 30 kN. In the transversal vibration, the outer surface of the upper plate (movable plate) was applied by a transversal displacement of 0.05 mm. The contact states were obtained when the transversal force approached the extreme to the left at each cycle. Figure 7(b) shows four contact states of thread surfaces at the position of the maximum transversal force. We can find that minor slippage propagates and develops to local slippage with the increase in vibration cycles, demonstrating the radial slippage propagation theory.

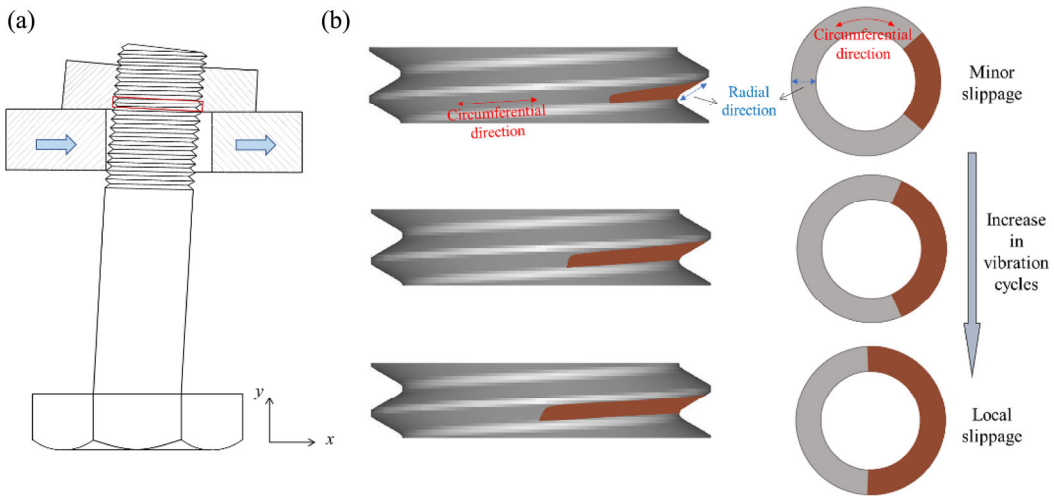

Fig. 5 Schematic of the radial slippage propagation theory: (a) bolted joint subjected to cyclic transversal vibration; (b) slippage propagation on the bearing and thread surfaces.

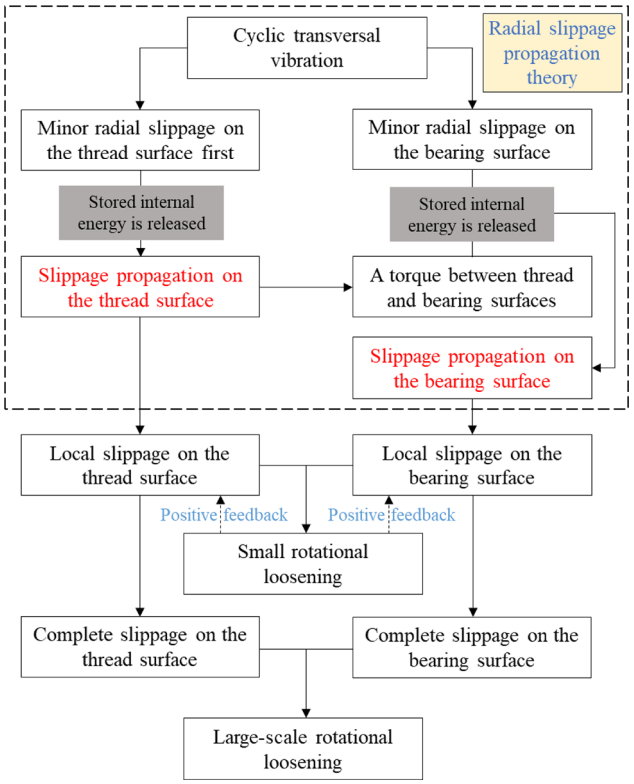

Fig. 6 Complete self-loosening process.

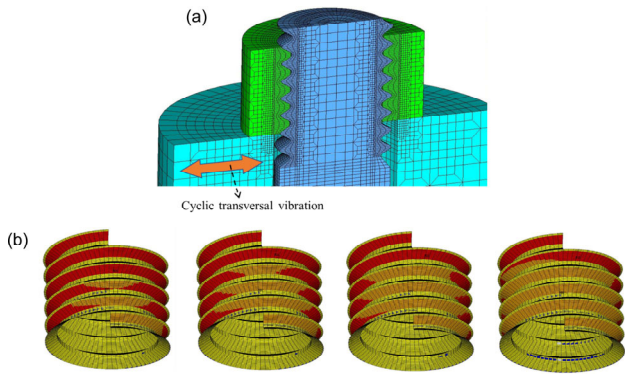

Fig. 7 FE simulation of a bolted joint subjected to cyclic transversal vibration: (a) 3D FEM of a regular bolted joint; (b) changes in contact states with increasing vibration cycles.

4 Innovative anti-loosening structure and performance evaluation

Based on the proposed radial slippage propagation theory, it is found that the key to anti-loosening is to prevent the occurrence of a relative motion of the external and internal threads in the radial direction under vibration, and thus to block slippage propagation. In this section, an innovative anti-loosening structure with step external and internal threads is proposed. The profile of the engagement between the step external and internal threads is presented in Fig. 8. We can observe that the original thread surface is divided into two sections by the step surface in the novel thread structure. The angle between the step surface and the original thread surface is defined as the step angle, which is designed to be 120°. As shown in Fig. 9(a), the occurrence of relative slippage of the external and internal threads in the radial direction becomes difficult owing to the step surface. Even though the initial relative slippage occurs under severe vibration, the negative feedback inhibits further slippage propagation and improves the anti-loosening ability. This is because the rise of the step external thread caused by the relative slippage will result in an increase of the preload and contact between the non-stress thread surfaces, as shown in Fig. 9(b).

In the novel thread structure, a proper step angle is important to ensure the excellent anti-loosening performance. Figure 10 shows the thread profiles for the step angles of 90° and 150°. When the step angle is 90°, it is obvious that the step surface plays a better role in preventing relative slippage between the external and internal threads than that at 120°. However, the stress concentration may be more remarkable, which increases the risk of bolt fatigue failure under cyclic vibration. Moreover, the processing of manufacturing of such step thread is complicated. When the step angle is 150°, the manufacturing process becomes simple. However, it is possible that the relative slippage on the step surfaces occurs more easily under cyclic vibration, which causes the failure of the anti-loosening

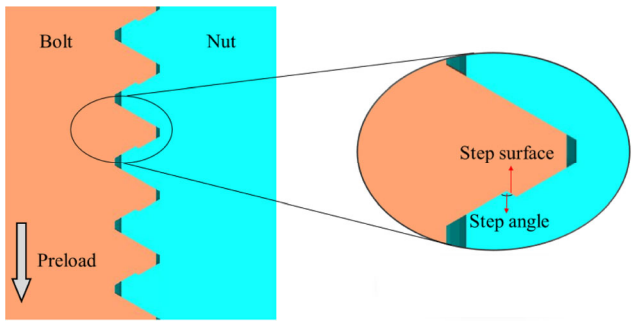

Fig. 8 Profile of the engagement between step internal and external threads.

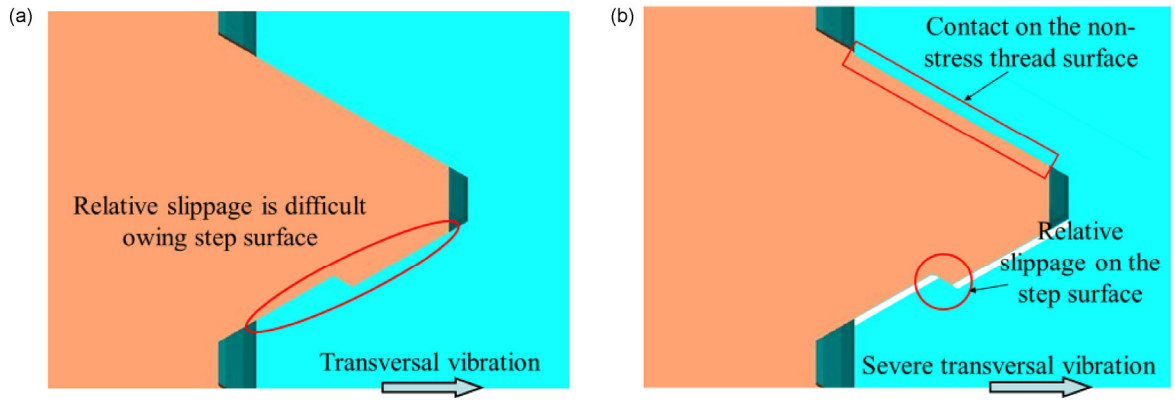

Fig. 9 Anti-loosening principle of innovative thread structure: (a) Relative slippage is difficult owing to step surface; (b) slippage propagation is inhibited due to the contact of non-stress thread surfaces.

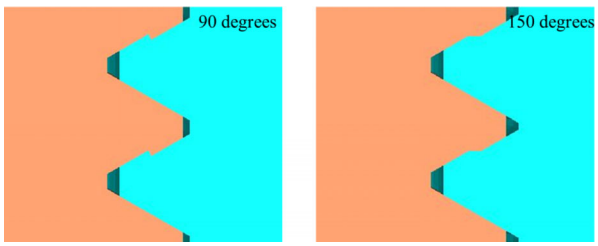

Fig. 10 Thread profiles for the step angels with 90° and 150°.

performance. In Section 4.1, we verify that a step angle of 120° is a reasonable selection.

4.1 Numerical analysis of step thread structure

In this section, FEMs of bolted joints with step threads and normal threads are established, as shown in Fig. 11. In the models, 3D meshes of external and internal

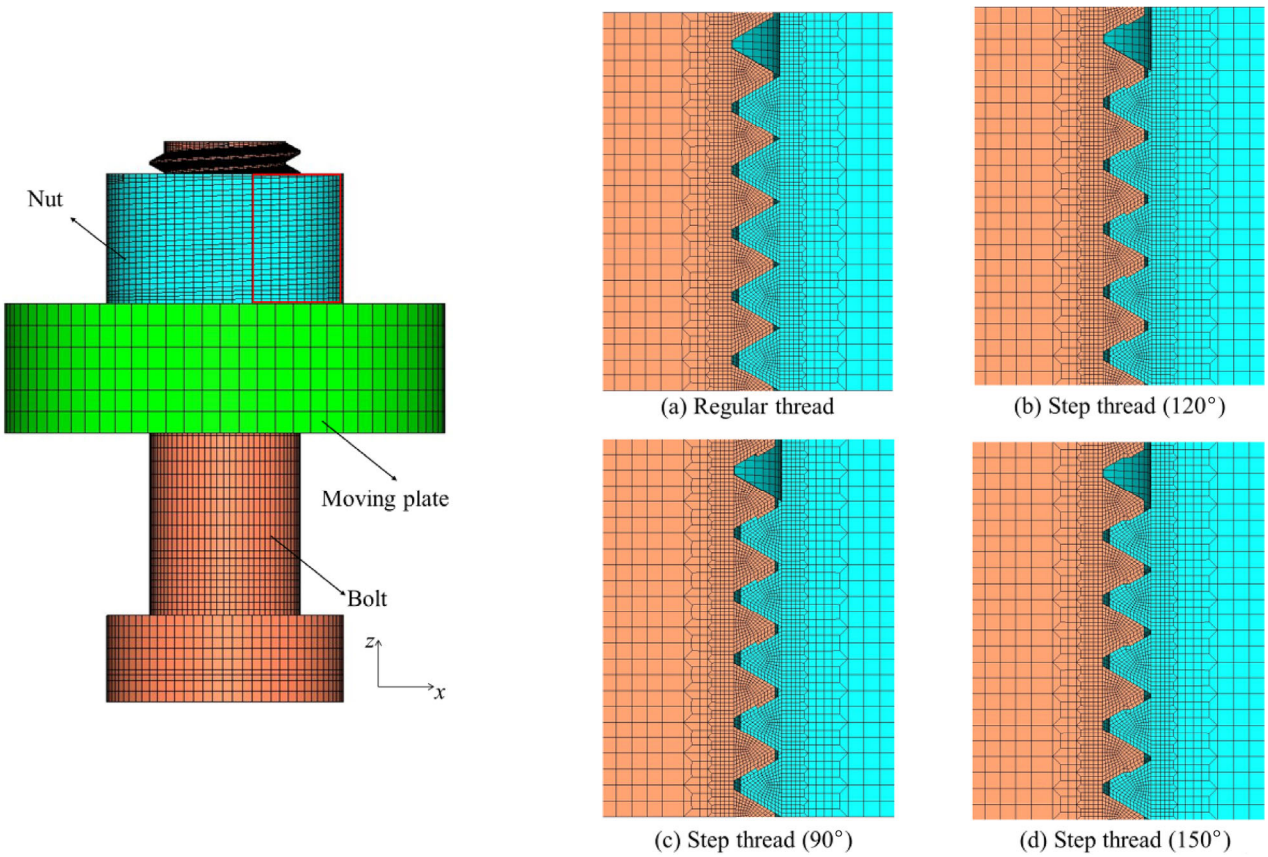

Fig. 11 FEMs of bolted joints with step threads and normal threads.

threads were built by rotating a two-dimensional cross-section of a thread spirally around the axis. Most of the 3D meshes were hexahedral, and the remaining meshes were triangular prisms. For the bolt model, a small hole appeared unavoidably, which was validated to have little influence on the result [22]. Additionally, the nut and bolt head were built to cylinders instead of hexagonal prisms for the convenience of meshing. The above meshing process was conducted by HyperMesh 12.0®, while the subsequent FEA was conducted by Ansys 16.0®. The FE model parameters are presented in Table 1. Plasticity is not considered in the present study. We only considered two pairs of contact interfaces: the contact surface of the external and internal threads and the bearing surface between the moving plate and the nut. One pair of contact interfaces were divided into target and contact surfaces, meshed by the TARGE 170 and CONTA 173 elements. The contact analysis used the augmented Lagrange method. The friction coefficients of all the contact interfaces were set to 0.15.

The preload was generated using the PRETS 179 pretension element [10, 19]. Bolted joints with grade 10.9 were applied, and the maximum preload achieving the yield limit of the material was approximately 50 kN. Three different preloads, 30, 35, and 40 kN, equalled 60%, 70%, and 80% of the maximum preload, respectively. A transversal displacement of 0.3 mm was employed to the outer surface of the movable plate. The vibrational cycle was set to 30. The bolt head surface was completely restrained, and the bottom of the movable plate was free and constrained in the y and z directions. Figure 12(a) shows the changes of preload as the number of vibration cycles is increased for bolted joints with normal threads and step threads (step angle = 120°). It can be observed that the preloads in the regular bolted joints decrease gradually, while those in the bolted joints with novel threads remain almost unchanged. This demonstrates the superior anti-loosening performance of the step

Table 1 FEM parameters.

Item	Value
Element type	Solid 185
Young's modulus	206 GPa
Poisson's ratio	0.3
Friction coefficient	0.15

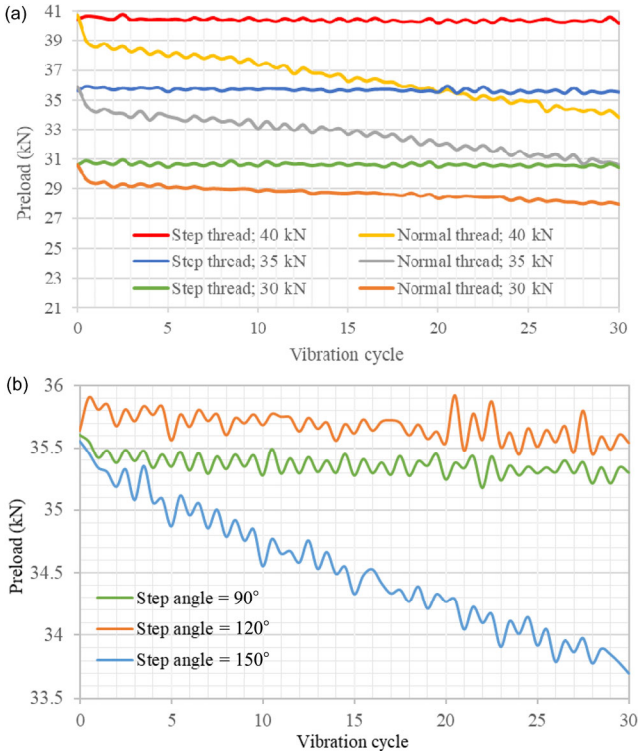

Fig. 12 Changes of preload as the number of vibration cycles is increased for bolted joints with normal threads and step threads: (a) different preloads; (b) different step angles.

thread structure compared to the normal one. A preload of 35 kN was also applied to the novel bolted joint with step angles of 90° and 150°, and a cyclic transversal vibration was simulated. Figure 12(b) presents the changes in the preloads in the bolted joints with different step angles. It can be observed that the bolted joints with step angles of 90° and 120° have unchanged tightening states (the preloads are not reduced) as the number of vibration cycles is increased, whereas the preload in the bolted joint with a step angle of 150° decreased gradually.

It has been reported that the bolt thread root located within one pitch of the nut-loaded surface has the maximum stress, where the fatigue fracture occurs most easily [36]. The root points (shown in Fig. 13) in the regular bolt and three novel bolts with different step threads were extracted, and their average stresses within a complete vibration cycle were analysed, presented in Fig. 14. From the hysteresis curves, we can find that the average stresses in the novel bolts with step angles of 120° and 150° range from 421 to 3,404 N and from 403 to 3,351 N, respectively, within a vibration cycle, whereas the average stress in the bolt

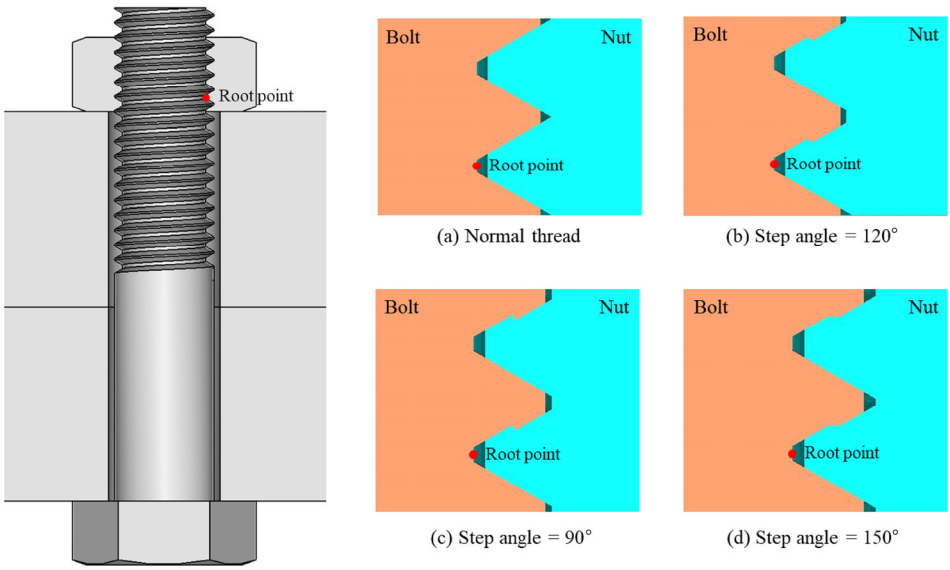

Fig. 13 Root points of the first engaged thread in the regular bolt and novel bolts with different step threads.

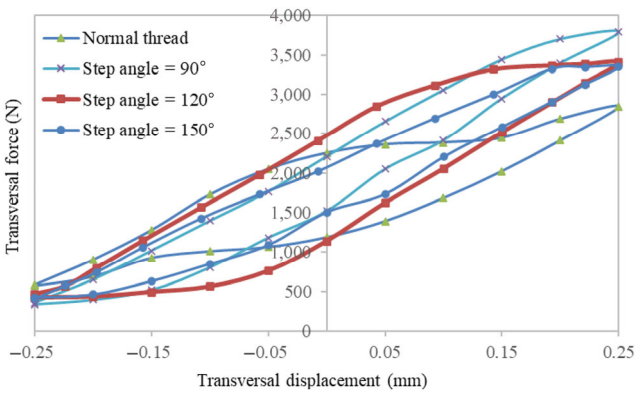

Fig. 14 Relationships between the transversal forces and transversal displacements in the normal bolt and novel bolts with different step threads.

with a step angle of 90° ranges between 335 and 3,794 N within a vibration cycle. Therefore, the novel bolts with step angles of 120° and 150° have higher anti-fatigue performance than that with a step angle of 90°. The average stresses in the regular bolt are between 570 and 2,846 N within a vibration cycle; however, the preload decreases due to loosen, which may aggravate the fatigue failure.

For a bolted joint, Eq. (1) presents the typical torque–tension relationship:

$$T = F\left(\mu_b r_b + \frac{p}{2\pi} + \frac{\mu_t r_t}{\cos\beta}\right) \quad (1)$$

where F is the preload, T is the tightening torque, μ_t is the friction coefficient between threads, μ_b is the friction coefficient between the bolt head/nut and its bearing surface, β is the half of the thread profile angle, r_t is the effective thread contact radius, r_b is the effective bearing contact radius, and p is the pitch of the threads. The MPC 184 element method was applied to simulate the tightening processes of the regular and three novel bolted joints [19]. The torque–tension relationship curves were obtained by FEM and Eq. (1), as shown in Fig. 15. It can be observed that the discrete points obtained from the regular bolted joint, and the novel bolted joints with step angles of 120° and 150° are almost on the curve depicted by Eq. (1). However, the discrete points obtained from the novel bolted joint with a step angle of 90° were slightly above the curve. This indicates that the novel bolted joint with a step angle of 90° is more difficult to tighten compared with the other step-thread structures. In conclusion, the FEA demonstrates that our proposed novel bolted joint with a step angle of 120° is advantageous in terms of anti-loosening, anti-fatigue, and tightening convenience.

In the previous study [22], we designed two types of thread structures, as shown in Fig. 16. Their anti-loosening and tightening performances were compared with those of several typical anti-loosening products using FEA. It was demonstrated that the

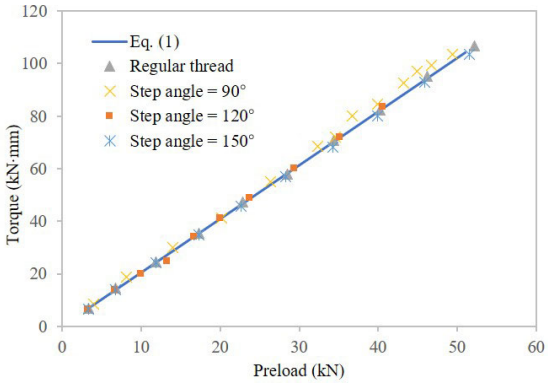

Fig. 15 Comparison of torque–tension relationships by FEM with Eq. (1).

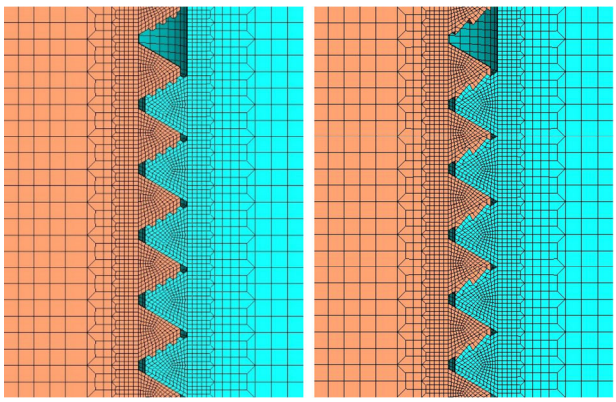

Fig. 16 Two thread connections designed in the previous paper [22]: (a) trapezoidal thread; (b) hook thread.

designed thread structures could be installed and removed conveniently, and they showed excellent anti-loosening performance. However, their anti-fatigue performances were not analysed. Herein, we applied the same method to compare the anti-fatigue performance of the thread structures designed in the previous paper with our proposed step thread structure by FEA. Figure 17 presents the results. The average stress within a cycle in the trapezoidal thread ranges from 207.34 to 4,085.99 N, whereas that in the hook thread is between 223.79 and 3,783.95 N. Obviously, the maximum stresses and variation ranges were both larger than those in the step thread. In other words, our proposed step thread has a better anti-fatigue performance.

4.2 Experimental study of step thread structure

To further validate the superior anti-loosening and anti-fatigue performance of bolted joints with step

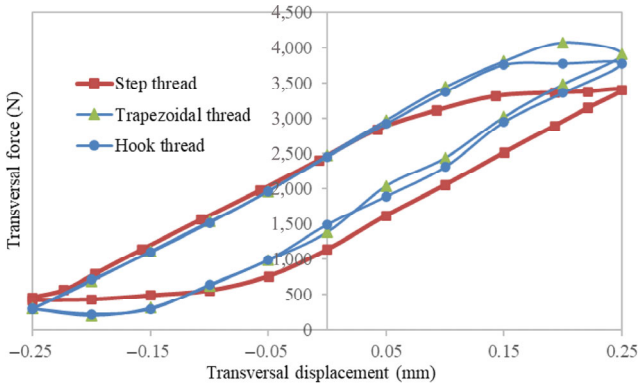

Fig. 17 Relationships between transversal forces and transversal displacements under different thread structures.

thread, and its convenience in installing and removing, vibration and tightening experiments were conducted. Figure 18 shows the design drawing of the step external and internal threads. The nominal diameter and pitch of the bolt and nut were 16 and 2 mm, respectively. Steel #1045 was used as the material. It is difficult for the existing tools to machine step internal and external threads. Two new tools with special angles were first manufactured, with which the novel bolted joint with a step thread could be produced. The surfaces of the bolt and nut require a blackening treatment after machining. We also manufactured regular bolts and nuts based on the same technology and materials for comparison. Figure 19(a) shows the novel bolted joint machined based on the design drawing and the regular bolted joint. Figure 19(b) shows the section profile of the step external and internal threads, while Fig. 19(c) shows the section profile of normal external and internal threads.

First, the tightening performance of a normal bolted joint and the novel bolted joint with a step thread was compared experimentally. A test equipment (a torque–tension machine (QBN-CN 500-500, Qianbang Test Equipment Co., Ltd., China)) was used to tighten various bolted joints and evaluate their tightening difficulties, as shown in Fig. 20. The tightening speed was maintained as a constant. A detailed experimental process can be found in the literature [22]. Each bolted joint was retightened three times, and the averages were calculated. The relationship curves between the input torque and preload are depicted in Fig. 21 based on the discrete testing data. From the figure, we can observe that the curve of the step thread is slightly

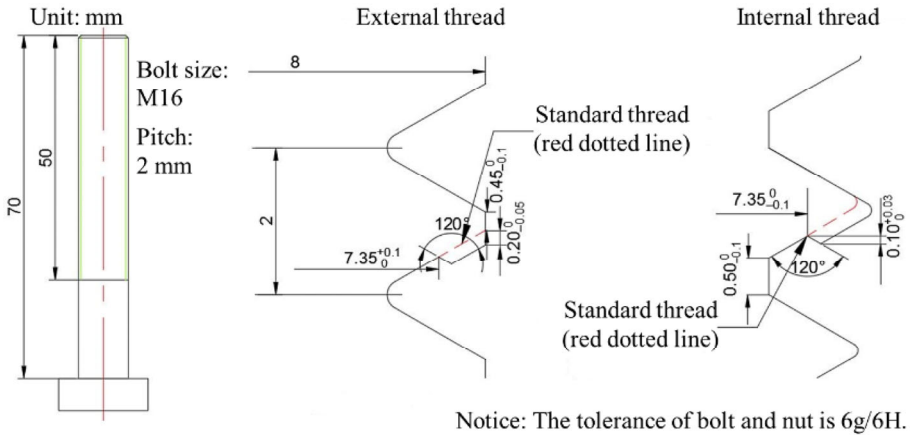

Fig. 18 Design drawing of step internal and external threads.

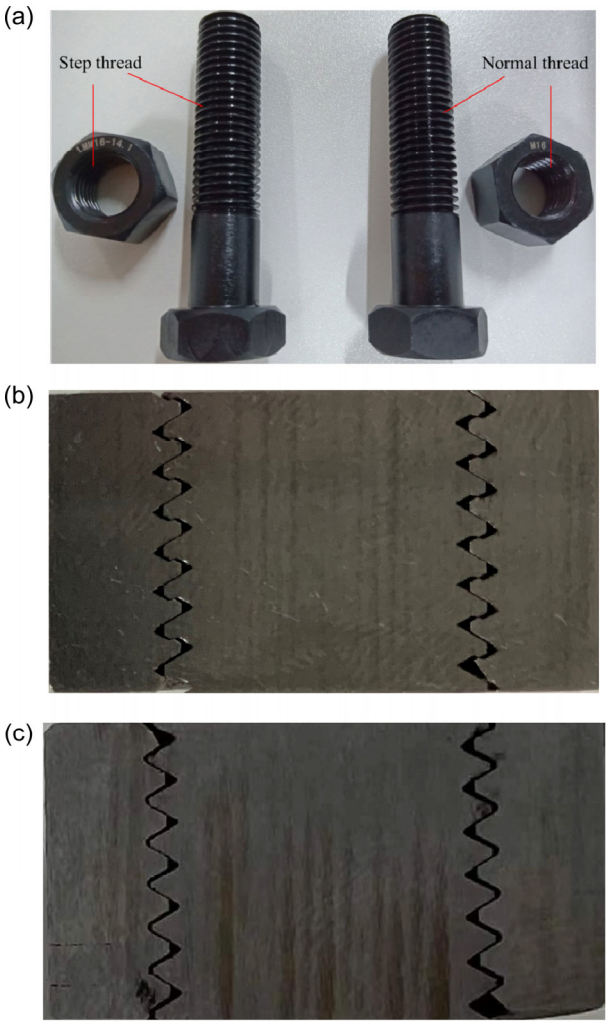

Fig. 19 Manufactured novel and regular bolted joints, and section profiles of the engagement threads: (a) novel and regular bolted joint; (b) section profile of step external and internal threads; (c) section profile of the normal external and internal threads.

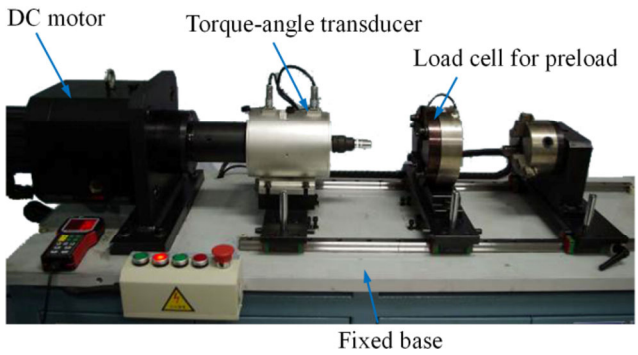

Fig. 20 Torque–tension test machine. Reproduced with permission from Ref. [22], © Elsevier Ltd. 2020.

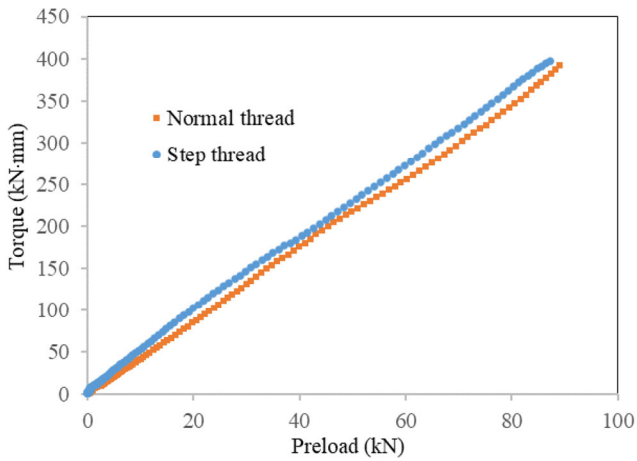

Fig. 21 Relationship curves between the input torque and preload.

steeper than that of the normal thread. The slopes of the fitted lines for the two curves are calculated to be 4.524 mm and 4.305 mm. The difference between these values is only 5%. Therefore, it can be concluded that the novel bolted joint with a step thread has a

tightening difficulty similar to that of the normal joint. Compared with other existing anti-loosening structures, such as wedge self-locking nuts and eccentric double nuts, the proposed thread structure can be installed and disassembled with great convenience.

Further, a transversal vibration equipment (the Junker test machine shown in Fig. 22) was applied to generate the cyclic vibration to the bolted joints and evaluate the anti-loosening and anti-fatigue performances of various bolted joints. The detailed experimental process can be found in the international standard [37]. The nut was tightened to the target preload of 50 kN. A small shear force of 2,500 N, produced by an eccentric structure, was first employed to the plate between the bolt and nut. The changes of preloads with an increase of vibration cycles can be obtained based on the measured data, as shown in Fig. 23(a). We can clearly see that the preload in the novel bolted joint is reduced slowly (almost unchanged), whereas that in the normal bolted joint decreases sharply. This demonstrates that our proposed bolted joint with a step thread has excellent anti-loosening ability. Furthermore, a large shear force of 6,000 N was employed to the plate. Figure 23(b) shows the changes of the preloads as the number of vibration cycles is increased. It can also be observed that the preload in the normal bolted joint decreases initially and vanishes (drops to 0) owing to bolt fatigue fracture after 7,500 vibration cycles. However, the novel bolted joint with a step thread is fractured owing to fatigue failure after 13,500 vibration cycles. Therefore, the novel bolted joint has advantages in terms of improving the anti-fatigue performance. It should be noted that the novel bolted joint loosens under large transversal vibrations. This may be because the thread wear and plastic deformation due to violent vibration cause the step thread to lose its ability to prevent radial slippage.

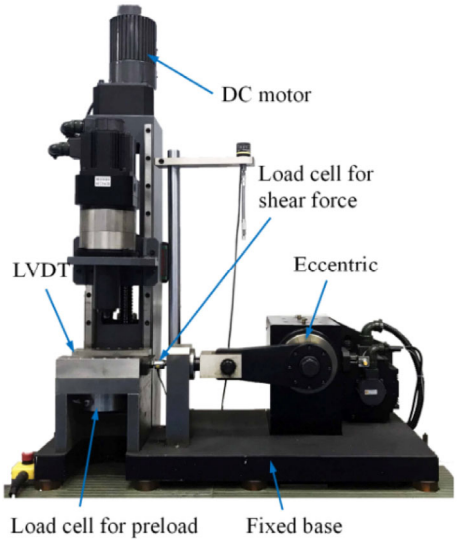

Fig. 22 Junker test machine. Reproduced with permission from Ref. [22], © Elsevier Ltd. 2020.

5 Comparison with Spiralock thread

Spiralock thread form as an anti-loosening structure has a modified thread profile including a 30° wedge ramp, as shown in Fig. 24 [30]. After the Spiralock nut is tightened, the tip of the regular bolt will be embedded into the wedge ramp. Essentially, this embedment will block the relative slippage between internal and external threads along the radial direction, and thus to prevent radial slippage propagation and

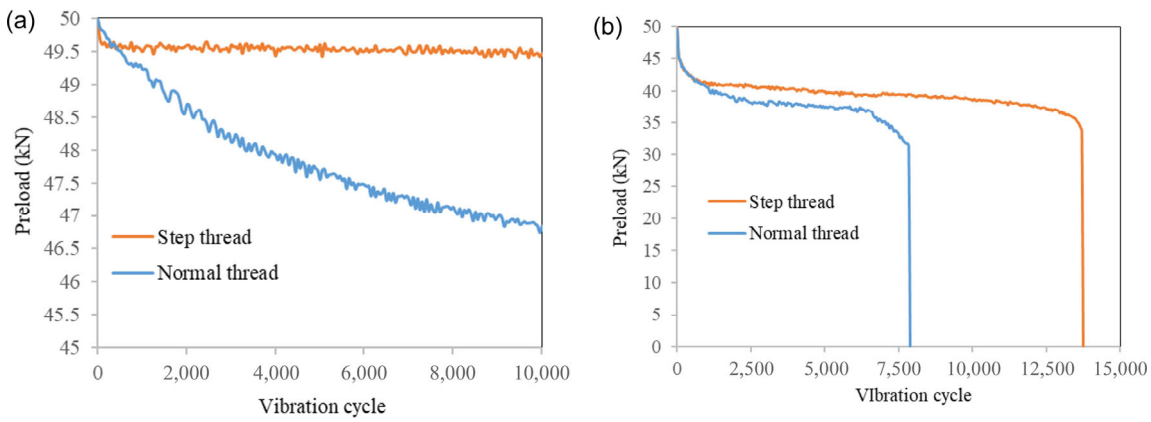

Fig. 23 Changes in preload with the increase in vibration cycles: (a) small amplitude; (b) large amplitude.

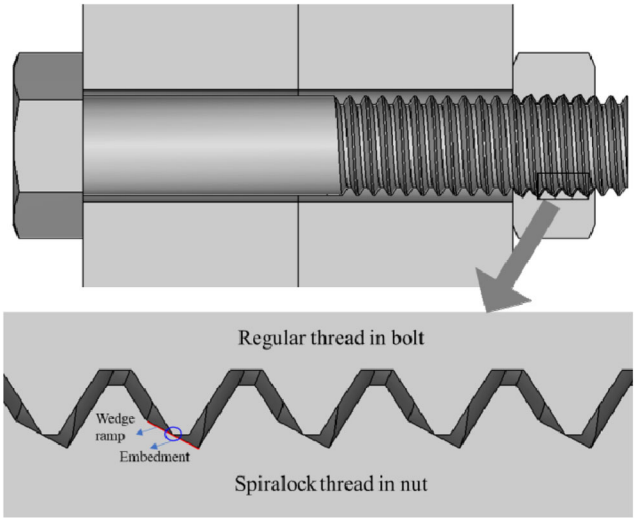

Fig. 24 Schematic of engagement between regular thread in bolt and Spiralock thread in nut.

loosening proceeding. In addition, the load distribution amongst engaged threads is more uniform, which is also helpful to improve the resistance to loosening. Subsequently, the tightening and anti-loosening performances of Spiralock thread form are compared with those of the step thread.

An FEM of engagement between regular bolt and Spiralock nut was built based on the method proposed by Liu et al. [30], as shown in Fig. 25. The model parameters are the same with those in Section 4.1. The MPC 184 element method was also used to simulate the tightening processes of nuts. The values of preloads and torques were extracted during the tightening process, and Fig. 26 presents the result. We can see that our proposed step thread almost has the same slope with the regular bolted joint while the Spiralock thread has a larger slope. It indicates that Spiralock nut is hard to be tightened, i.e., an

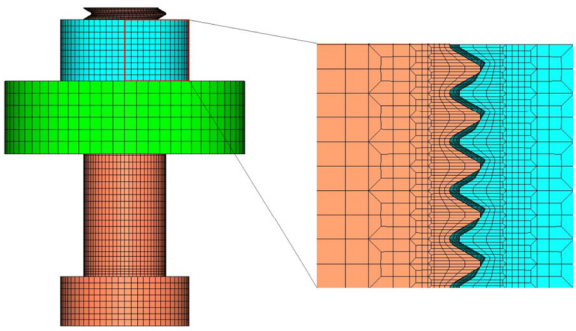

Fig. 25 FEM of engagement between regular bolt and Spiralock nut.

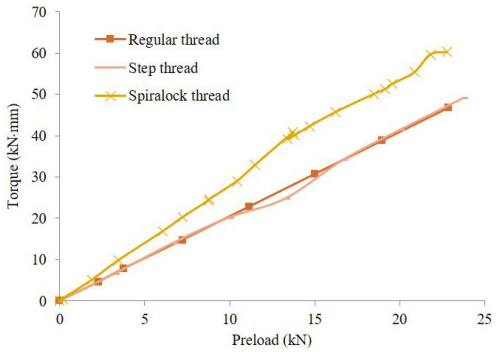

Fig. 26 Relationship curves between the input torque and preload in three types of threaded connections.

additional torque will be required for a Spiralock nut to obtain the same preload.

To evaluate the anti-loosening performance, a cyclic transversal vibration with the amplitude of 0.3 mm was simulated. The vibrational cycle was set to 30. In the simulation, the initial preloads were set to 3 and 30 kN. Figure 27 shows the changes of preloads with the increase of vibrational cycles. We can see from Fig. 27(a) that when the initial preload is large (30 kN), there is little change in preloads under transversal vibration, i.e., Spiralock and step threades both have great anti-loosening abilities. When the initial preload

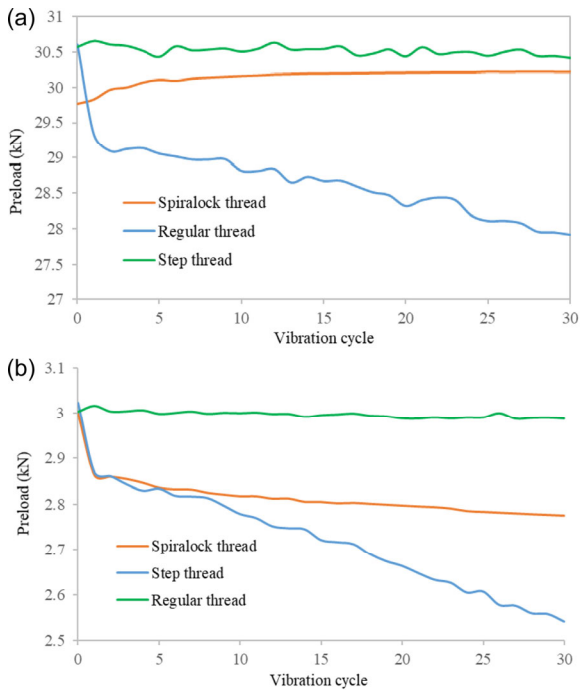

Fig. 27 Changes in preload with the increase in vibration cycles for Spiralock and step threads: (a) large initial preload; (b) small initial preload.

is small (3 kN), the result is different. It can be found clearly from Fig. 27(b) that the preload in Spiralock thread is reduced quickly, whereas that in step thread is almost unchanged. Therefore, Spiralock thread may lose anti-loosening ability when the initial preload is small, which has been validated by Liu et al. [30]. However, our proposed step thread shows excellent resistance to loosen.

In summary, Spiralock thread form is harder to be tightened for the same preload and will lose the anti-loosening performance when the initial preload is small compared with our proposed step thread. It indicates that our step thread shows more excellent tightening and anti-loosening performances.

6 Future research work

This paper proposes a radial slippage propagation theory that triggers self-loosening. The reliability of the novel theory is validated using FEA. However, effective experimental validation is lack. In the future, it is essential to apply advanced measurement methods to observe the actual contact states on the bearing and thread surfaces, especially when the bolted joint is subjected to the cyclic transversal vibration. Consequently, the evolution of the contact states on the contact surfaces can be revealed for the experimental validation of the radial slippage propagation theory. For the proposed novel bolted joint with step thread, the experimental results indicate that large vibrations may cause material wear on the thread surface, and thus decrease the anti-loosening ability. Therefore, the material, shape, angle, size, and tolerance of the step-thread structure need to be optimised and further investigated in future research. Many experiments should be conducted to evaluate their performance before practical applications. Moreover, the development of a simple method to machine the step internal and external threads is also a key issue worthy of future research.

7 Conclusions

This paper proposes a radial slippage propagation theory to reveal the self-loosening process of a bolted joint subjected to cyclic transversal vibration. In contrast to the traditional complete slippage theory and local slippage accumulation theory, the new theory states that slippage along the radial direction of the thread surface can induce more slippage areas (slippage propagation) on the thread surfaces, and self-loosening occurs owing to the dynamic evolution and propagation of contact states on the bearing and thread surfaces with the increase of the vibration cycles. It was found that minor slippage with a small constant-sticking area within a complete vibration cycle at the initial vibration cycles can expand to local slippage and complete slippage with an increase of vibration cycles, and finally result in continuous self-loosening. A novel anti-loosening structure with step internal and external threads was developed, with which slippage propagation on the thread surface could be prevented. Its excellent anti-loosening and anti-fatigue performances, as well as the convenience of installation and removal, were validated by FEA and experiments. In the future, advanced measurement methods should be explored to observe the actual contact states on the bearing and thread surfaces to validate the radial slippage propagation theory experimentally. Furthermore, the step thread structure requires further optimisation, including the shape, angle, size, and tolerance.

Declaration of competing interest

The authors have no competing interests to declare that are relevant to the content of this article.

Acknowledgements

This work was supported by the National Natural Science Foundation of China (Grant Nos. 51935003 and 52105503) and China Postdoctoral Science Foundation (Grant No. 2021M690396).

References

[1] Li Q Y, Zhao Y, Sun Q C, Chen K Y. Reliability evaluation method of anti-loosening performance of bolted joints. *Mech Syst Signal Pr* **162**: 108067 (2021)

[2] Towsyfyan H, Gu F S, Ball A D, Liang B. Tribological behaviour diagnostic and fault detection of mechanical seals based on acoustic emission measurements. *Friction* **7**(6): 572–586 (2019)

[3] Zhou J B, Liu J H, Ouyang H J, Cai Z B, Peng J F, Zhu M H. Anti-loosening performance of coatings on fasteners subjected to dynamic shear load. *Friction* **6**(1): 32–46 (2018)

[4] Information on https://news.sohu.com/20100709/n273386423.shtml, 2010. (in Chinese)

[5] Gong H, Ding X Y, Liu J H, Feng H H. Review of research on loosening of threaded fasteners. *Friction* **10**(3): 335–359 (2022)

[6] Dong Y D, Li Y. Reliability of roof panels in coastal areas considering effects of climate change and embedded corrosion of metal fasteners. *ASCE-ASME Journal of Risk and Uncertainty in Engineering Systems A* **2**(1): 04015016 (2016)"

[7] Abboud A, Nassar S A. Viscoelastic strain hardening model for gasket creep relaxation. *J Press Vessel Technol* **135**(3): 031201 (2013)

[8] Guo J Q, Zheng X T, Zhang Y, Shi H C, Meng W Z. A unified continuum damage mechanics model for predicting the stress relaxation behavior of high-temperature bolting. *J Press Vessel Technol* **136**(1): 011203 (2014)

[9] Jiang Y Y, Zhang M, Lee C H. A study of early stage self-loosening of bolted joints. *J Mech Des* **125**(3): 518–526 (2003)

[10] Gong H, Liu J H, Ding X Y. Study on the mechanism of preload decrease of bolted joints subjected to transversal vibration loading. *Proc Inst Mech Eng B J Eng Manuf* **233**(12): 2320–2329 (2019)

[11] Zhang M Y, Zeng D F, Lu L T, Zhang Y B, Wang J, Xu J M. Finite element modelling and experimental validation of bolt loosening due to thread wear under transverse cyclic loading. *Eng Fail Anal* **104**: 341–353 (2019)

[12] Zhang M Y, Lu L T, Wang W J, Zeng D F. The roles of thread wear on self-loosening behavior of bolted joints under transverse cyclic loading. *Wear* **394–395**: 30–39 (2018)

[13] Junker G H. New criteria for self-loosening of fasteners under vibration. *SAE Trans* **78**(1): 314–335 (1969)

[14] Goodier J N, Sweeney R J. Loosening by vibration of threaded fastenings. *Mech Eng* **67**: 798–802 (2022)

[15] Pai N G, Hess D P. Experimental study of loosening of threaded fasteners due to dynamic shear loads. *J Sound Vib* **253**(3): 585–602 (2002)

[16] Pai N G, Hess D P. Three-dimensional finite element analysis of threaded fastener loosening due to dynamic shear load. *Eng Fail Anal* **9**(4): 383–402 (2002)

[17] Izumi S, Yokoyama T, Iwasaki A, Sakai S. Three-dimensional finite element analysis of tightening and loosening mechanism of threaded fastener. *Eng Fail Anal* **12**(4): 604–615 (2005)

[18] Izumi S, Kimura M, Sakai S. Small loosening of bolt-nut fastener due to micro bearing-surface slip: A finite element method study. *J Solid Mech Mater Eng* **1**(11): 1374–1384 (2007)

[19] Gong H, Liu J H. Some factors affecting the loosening failure of bolted joints under vibration using finite element analysis. *Proc Inst Mech Eng C J Mech Eng Sci* **232**(21): 3942–3953 (2018)

[20] Dinger G, Friedrich C. Avoiding self-loosening failure of bolted joints with numerical assessment of local contact state. *Eng Fail Anal* **18**(8): 2188–2200 (2011)

[21] Gong H, Liu J H, Ding X Y. Thorough understanding on the mechanism of vibration-induced loosening of threaded fasteners based on modified Iwan model. *J Sound Vib* **473**: 115238 (2020)

[22] Gong H, Liu J H, Ding X Y. Study on local slippage accumulation between thread contact surfaces and novel anti-loosening thread designs under transversal vibration. *Tribol Int* **153**: 106558 (2021)

[23] Gong H, Liu J H, Feng H H. Review on anti-loosening methods for threaded fasteners. *Chin J Aeronaut* **35**(2): 47–61 (2022)

[24] Izumi S, Kimura M, Sakai S. Evaluation of loosening proof performance of plain washer and flange nut by three-dimensional finite element analysis. *Trans JSME Ser A* **72**(721): 1292–1295 (2006) (in Japanese)

[25] Kimura M, Izumi S, Sakai S. Self-loosening behaviour of a spring washer: Three-dimensional finite element method study. *Trans JSME Ser A* **73**(734): 1105–1110 (2007) (in Japanese)

[26] Yokoyama T, Oishi K, Kimura M, Izumi S, Sakai S. Evaluation of loosening resistance performance of conical spring washer by three-dimensional finite element analysis. *J Solid Mech Mater Eng* **2**(1): 38–46 (2008)

[27] Liu J H, Gong H, Ding X Y. Anti-loosening performance of wedge washers under vibration. *J Vib Shock* **38**(5): 38–44, 70 (2019) (in Chinese)

[28] Izumi S, Yokoyama T, Kimura M, Sakai S. Loosening-resistance evaluation of double-nut tightening method and spring washer by three-dimensional finite element analysis. *Eng Fail Anal* **16**(5): 1510–1519 (2009)

[29] Sawa T, Ishimura M, Karami A. A bolt-nut loosening mechanism in bolted connections under repeated transverse loadings (effect of inclined bearing surfaces on the loosening). In: Proceedings of the ASME 2010 Pressure Vessels and Piping Division/K-PVP Conference, Bellevue, USA, 2010: 397–403.

[30] Liu J H, Gong H, Ding X Y. Effect of ramp angle on the anti-loosening ability of wedge self-locking nuts under vibration. *J Mech Des* **140**(7): 072301 (2018)

[31] Eccles W, Sherrington I, Arnell R D. Towards an understanding of the loosening characteristics of prevailing torque nuts. *Proc Inst Mech Eng C J Mech Eng Sci* **224**(2): 483–495 (2010)

[32] Ranjan B S C, Vikranth H N, Ghosal A. A novel prevailing torque threaded fastener and its analysis. *J Mech Des* **135**(10): 101007 (2013)

[33] Sase N, Nishioka K, Koga S, Fujii H. An anti-loosening screw-fastener innovation and its evaluation. *J Mater Process Technol* **77**(1–3): 209–215 (1998)

[34] Sase N, Fujii H. Optimizing study of SLBs for higher anti-loosening performance. *J Mater Process Technol* **119**(1–3): 174–179 (2001)

[35] Sun Q C, Lin Q Y, Yang B, Zhang X L, Wang L T. Mechanism and quantitative evaluation model of slip-induced loosening for bolted joints. *Assembly Autom* **40**(4): 577–588 (2020)

[36] Fukuoka T, Nomura M. Proposition of helical thread modeling with accurate geometry and finite element analysis. *J Press Vess Technol* **130**(1): 011204 (2008)

[37] ISO 16130. Aerospace series-dynamic testing of the locking behavior of bolted connections under transverse loading conditions (vibration test). ISO, 2015.

Hao GONG. He received his Bachelor degree in mechanical engineering in 2014 from Beijing Institute of Technology, Beijing, China. After then, he was a Ph.D. student in the Digital Manufacturing Laboratory at the same university. He obtained his Ph.D. degree in mechanical engineering in March 2020 and now he is a postdoctor at Beijing Institute of Technology. His research interests include high-performance assembly and high-reliability assembly for threaded fasteners.

Jianhua LIU. He received his M.S. degree in mechanical engineering in 2002 from Chongqing University, Chongqing, China, and received his Ph.D. degree in the same major in 2005 from Beijing Institute of Technology, Beijing, China. After then, He joined the Digital Manufacturing Laboratory at Beijing Institute of Technology. His current position is Professor and Vice President of Graduate School. His research areas cover digital manufacturing, precision assembly, and measurement.